Local fringe density determination by adaptive filtering

J. Vargas,[1,*] J. Antonio Quiroga,[2] and T. Belenguer[1]

[1]*Laboratorio de Instrumentación Espacial, Instituto Nacional de Técnica Aeroespacial, Carretera de Ajalvir Km 4, 28850, Torrejón de Ardoz, Madrid, Spain*

[2]*Optics Department, Universidad Complutense de Madrid, Facultad de CC. Físicas, Ciudad Universitaria s/n, 28040 Madrid, Spain*

**Corresponding author: jvargas@fis.ucm.es*

Received September 20, 2010; revised November 8, 2010; accepted November 13, 2010; posted December 3, 2010 (Doc. ID 135449); published December 27, 2010

We demonstrate a method to easily and quickly determine the local fringe density map of a fringe pattern. The method is based on an isotropic adaptive bandpass filter that is tuned at different frequencies. The modulation map after applying a specific bandpass frequencies filter presents a maximum response in the regions where the bandpass filter and fringe frequencies coincide. We show a set of simulations and experimental results that prove the effectiveness of the proposed method. © 2010 Optical Society of America

OCIS codes: 100.2650, 100.2000.

The local fringe density map (LFD) gives important information of a fringe pattern. On one hand, the LFD map is directly related to the strain tensor map [1]. On the other hand, the two most widely used algorithms for determining the orientation of a fringe pattern, gradient [2] and plane-fit methods [3], are highly affected by the so called "window choosing problem" [4]. This problem affects the precision of the computed fringe orientation considerably [5]. The window choosing problem influences, in fact, all fringe processing methods based on block processing. For example, in [5] is shown a single-frame demodulating algorithm based on a local adaptable quadrature filter. This method is based on processing into small areas where the fringe pattern is locally monochromatic; that is, locally there is a single spatial frequency. In [6] is presented a phase-shifting demodulating method based on dividing the interferograms into small regions, where the phase-shifting can be considered approximately constant; a self-calibrating approach is applied in each block. In [7] is shown the regularized phase tracker presented by Servín *et al.* In [7], it is necessary to specify a neighborhood region around each pixel to process. All the methods presented above are affected by the window choosing problem. The LFD map can be used to determining the appropriate window size for each pixel as a preprocessing step. To have a useful preprocessing algorithm, it is necessary that the algorithm be accurate and quick enough.

Currently there are some reported methods to retrieve the LFD map of a fringe pattern. Jun and Asundi [1] described a method to determine the LFD map based on selecting a bank of Gabor filters, whose responses cover one-half of the frequency plane, and constructing the output, taking into account the amplitude of the corresponding response. The problem of this method is that, since the passband of the filters must be narrow enough, this scheme requires too many filters to be of practical use. Another existing method to estimate the fringe density map of an interferogram is presented in [8]. In this work is shown a fringe density estimation method by continuous wavelet transform. The main drawbacks of this method are the required long computation times, computation complexity, and low accuracy results.

In this Letter, we propose an isotropic method for obtaining the LFD map in an easy-to-implement, fast, and accurate way. The algorithm is based on applying a set of bandpass filters tuned at different frequencies to the fringe pattern to process. For each bandpass filter, the resultant modulation map is obtained after applying it to the fringe pattern. Finally, for each pixel, the filter tuning frequency that gives the maximum modulation at that pixel is selected. The used isotropic bandpass filters that have annular frequency responses are shown in Fig. 1. As the filters have annular frequency response, the whole frequency plane must be completely covered using a set of filters that is not large. The filters shown in Fig. 1 can be expressed in polar coordinates as

$$H_k(\rho,\theta) = G(\rho - \rho_k) \tag{1}$$

where ρ is the modulus of the spatial frequency, θ is the polar angle, and $G(\rho)$ is a bell-shaped function with tuning frequency ρ_k. In this work, the function $G(\rho)$ is a typical Gaussian function given as

$$H_k(\rho,\theta) = \exp\left[-0.5\left(\frac{\rho-\rho_k}{\sigma}\right)^2\right]. \tag{2}$$

The Gaussian choice is a practical matter. Width and tuning frequency are parameters of the Gaussian, and it can be easily expressed in polar coordinates. Its space-frequency localization properties are well studied [9],

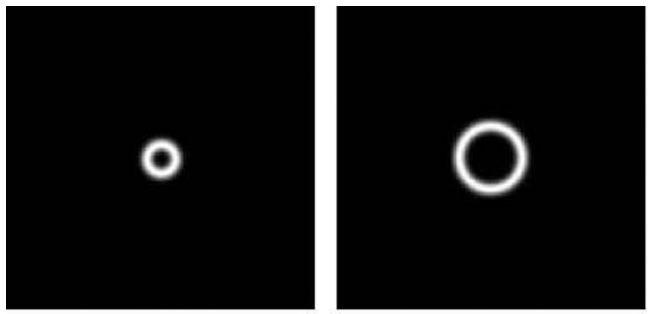

(a) (b)

Fig. 1. Isotropic bandpass filters tuned at different frequencies.

 © 2011 Optical Society of America

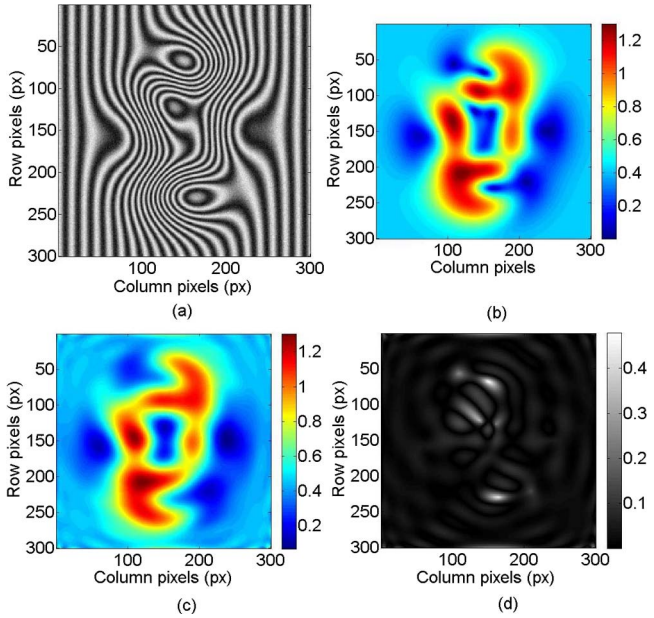

Fig. 2. (Color online) (a) 300 × 300 test pattern, (b) actual LFD map, (c) obtained LFD map, (d) absolute difference between the actual and obtained LFD maps. The main error comes from the low fringe density regions.

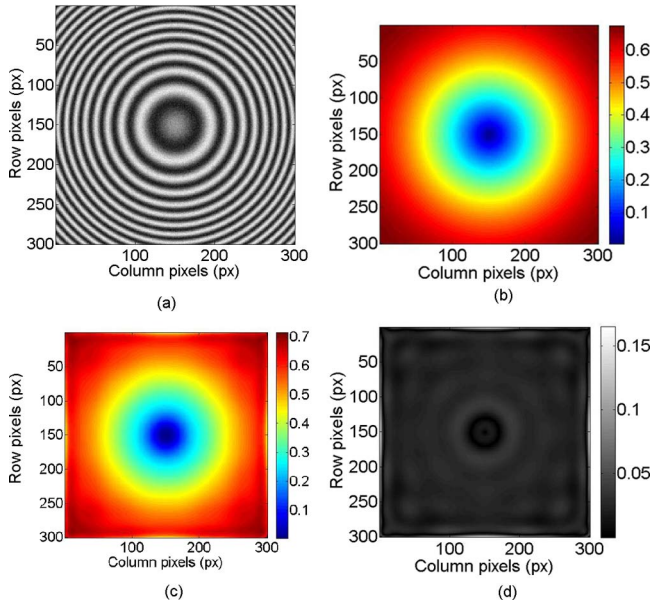

Fig. 3. (Color online) (a) 300 × 300 circular test interferogram, (b) actual LFD map, (c) obtained LFD map, (d) absolute difference between the actual and obtained LFD maps.

and its superposition properties makes the Gaussian a natural choice to sample the frequency space.

In Eq. (2), σ is proportional to the standard deviation and makes the filter wider or sharper. The resultant complex map (G_k) resulting from applying the filter H_k over the fringe pattern I is given by

$$G_k = \mathrm{IFT}((\mathrm{FT}[I]) \cdot H_k), \tag{3}$$

where FT denotes the two-dimensional Fourier transform and IFT denotes the inverse two-dimensional Fourier transform. The resultant modulation map is obtained from G_k as

$$M_k = \sqrt{\mathrm{Re}(G_k)^2 + \mathrm{Im}(G_k)^2}. \tag{4}$$

The modulation map is an important magnitude that weighs the goodness of the resultant local density fringe measurement [10]. In the regions where the fringe and the tuned filter frequencies are similar, the modulation map will present maxima values. Therefore, the LFD map can be obtained looking for the frequencies ρ_k that give a maximum response in the resultant modulation map. In this work, we have used a bank of filters composed by N filters with $N = 50$ and tuned at different frequencies. To minimize the interaction of the filter responses with the transformed image borders, we recommend selecting the last frequency radius so that the tails of the last Gaussian annulus are practically zero at the borders. Additionally, we recommend selecting the first frequency radius so that the tails of the Gaussian are nearly zero at the frequency origin. The reason is that the interferogram background is usually a smooth signal, and its spectrum overlaps with the interferogram spectrum for low spatial frequencies. The selection of the N and σ parameters depends on the application. In general, the N and σ parameters should be chosen so that the Gaussian superposition uniformly covers the frequency interval of interest.

The algorithm requires as input a rough estimation of the minimum ($\chi_{\min}$) and maximum ($\chi_{\max}$) fringes per field of the fringe pattern. The frequency step (s) between two consecutive tuning frequencies is given by $s = \frac{\chi_{\max} - \chi_{\min}}{N}$. In this work, σ is obtained from the frequency step as $\sigma = 15s$. If the maximum of modulation for a pixel is less than a cutoff value (typically, 0.3 over 1 of the normalized modulation), this pixel is filtered out. Finally, if desired, it is possible to perform a Zernike interpolation over the whole map.

Figures. 2 and 3 show the results obtained by the proposed method to two different simulated fringe patterns. Figure 2(a) shows the first simulated fringe pattern to process. This pattern is affected by white noise and has a 10% signal-to-noise ratio. Figures 2(b) and 2(c) show the actual and obtained local density maps respectively. Finally, Fig. 2(d) shows the absolute difference between the actual and obtained local density maps. The rms between the actual and obtained LFD maps is about 0.05 rad/px. The processing time necessary using the proposed method is 3.4 s using a laptop of 1.6 GHz and MATLAB. To study the performance of the algorithm in terms of N and σ, we have

Table 1. Root-Mean-Square Errors between the Actual and Obtained LFD Maps Computed from the Fringe Pattern Shown in Fig. 2(a) and for Different Values of N and σ

	$N = 15$	$N = 30$	$N = 50$	$N = 65$	$N = 80$
	rms (rad/px)				
$\sigma = 5s$	0.092	0.062	0.059	0.063	0.068
$\sigma = 10s$	0.10	0.065	0.052	0.050	0.051
$\sigma = 15s$	0.11	0.068	0.053	0.049	0.047
$\sigma = 30s$	0.12	0.076	0.060	0.054	0.052
$\sigma = 35s$	0.12	0.078	0.060	0.055	0.053

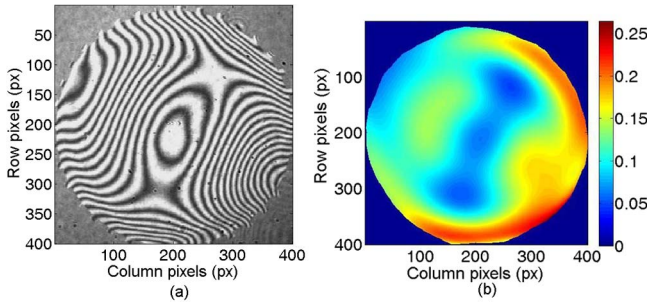

Fig. 4. (Color online) (a) 400×400 Fizeau interferogram, (b) obtained LFD map.

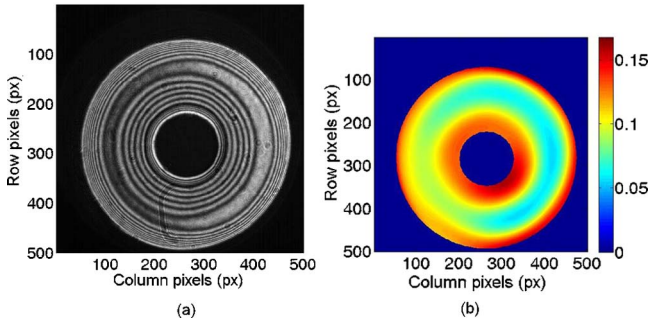

Fig. 5. (Color online) (a) 500×500 image of an annular specular surface, (b) obtained LFD map.

obtained the rms errors for different values of N and σ and for the fringe pattern shown in Fig. 2(a). The results are presented in Table 1. As can be seen from Table 1, the minimum rms value is obtained when $N = 50$ and $\sigma = 10s$; additionally, the rms errors shown in Table 1 have similar magnitude, so the results do not depend strongly on the selection of N and σ parameters. Figure 3(a) shows the second simulated fringe pattern to process composed by closed fringes. As in the previous fringe pattern, the pattern is affected by white noise with a 10% signal-to-noise ratio. Figures 3(b) and 3(c) show the actual and obtained LFD maps. Finally, Fig. 3(d) shows the absolute difference between the actual and obtained LFD maps. In this case, the rms error is about 0.025 rad/px, and the processing time is 3.3 s. In order to show the robustness of the proposed method, we have also tested it with experimental interferograms. Figures 4(a) and 5(a) show two real interferograms characterized by a wide spatial frequency spectrum. In both examples, the fringe pattern presents low and high spatial frequency regions together with noise, especially visible in the case of Fig. 5(a). Figures 4(b) and 5(b) show the resultant LFD maps obtained by our method. The processing time is about 10 s in both cases. As can be seen from Figs. 4(b) and 5(b), the obtained LFD are compatible with the interferogram fringe distribution.

Summarizing, we have presented an easy-to-implement, fast, and accurate method for obtaining the LFD map of a fringe pattern. Compared with exiting techniques, the proposed method is quick and fast in the sense that if N is the number of discrete spatial frequencies, our method uses N correlations; meanwhile, the filter bank [1] and wavelet [8] methods use $N \times N$ and $N \times N \times K$ correlations, respectively (assuming K discrete steps for the wavelet scaling). We have shown a set of results from simulated and real fringe patterns, and we have compared the obtained and actual LFD maps in the case of the simulated results obtaining satisfactory results.

References

1. W. Jun and A. Asundi, Appl. Opt. **41**, 7229 (2002).
2. M. Kass and A. Witkin, Comput. Vis. Graph. Image Process. **37**, 362 (1987).
3. X. Yang, Q. Yu, and S. Fu, Opt. Commun. **274**, 286 (2007).
4. S. Fu, H. Lin, J. Chen, and Q. Yu, Opt. Commun. **272**, 73 (2007).
5. J. C. Estrada, M. Servín, and J. L. Marroquín, Opt. Express **15**, 2288 (2007).
6. A. Dobroiu, D. Apostol, V. Nascov, and V. Damian, Appl. Opt. **41**, 2435 (2002).
7. M. Servín, J. L. Marroquin, and F. J. Cuevas, J. Opt. Soc. Am. A **18**, 689 (2001).
8. C. Quan, C. J. Tay, and L. Chen, Appl. Opt. **44**, 2359 (2005).
9. C. A. Sciammarella and K. Taeeeui, Opt. Eng. **42**, 3182 (2003).
10. B. Strobel, Appl. Opt. **35**, 2192 (1996).